

Investigating the impact of complex topography in sand dune areas on the application of static corrections in NC 210 seismic lines

Riyadh Alhajni*, Naser altoumi, Entsar haman, Salah Elgabir, Ali Milad Alghol

Faculty of oil and gas engineering, University of Zawia

*R.alhajni@zu.edu.ly, N.altoumi@zu.edu.ly, E.haman@zu.edu.ly, S.elgabir@zu.edu.ly, a.alghol@zu.edu.ly

Abstract

Sand dune interference poses significant challenges for seismic data acquisition and processing in the Murzuq Basin, southwestern Libya. The region's extensive sand dune fields introduce notable noise into seismic records, complicating data processing and generating spurious subsurface images. Additionally, the unique geomorphology of sand dunes, characterized by steep slopes and low seismic velocities, induces time delays in seismic wave propagation, resulting in distorted and inaccurate reflection data. To address these issues, a comprehensive reprocessing effort was undertaken on three seismic lines (202, 207, and 209), totaling 12 kilometers, at the Western Geco processing center in Tripoli using Omega software. The study focused on evaluating the efficacy of various gain correction techniques; including time function gain, geometric spreading, and residual amplitude analysis compensation (RAAC). In parallel, a comparative analysis of conventional uphole and elevation static methods were conducted. Preliminary findings suggest that the uphole method offers superior performance in mitigating static problems compared to the elevation method. A detailed assessment of the gain correction techniques is currently underway to determine their respective contributions to overall data quality improvement.

Keywords: Static Correction; Elevation Statics; Datum Statics; Seismic Processing; Sand Dunes Problems.

Introduction

Concession NC210, situated in the northwestern Murzuq Basin of western Libya, presents a formidable challenge for seismic exploration due to its harsh desert environment (Figure 1A). Seismic lines 202, 207, and 209 traverse this region, necessitating data acquisition across complex dune topography—typically 1.5 kilometers wide and 100 meters high. Seismic surveys in this area commenced in 1960, employing weight drops and dynamite as initial seismic sources. More recent explorations have predominantly utilized vibriosis, although dynamite remains a supplementary source in certain locations.

The Atchan field, situated east of the study area, has undergone extensive drilling. Notably, well F1-NC210, a wildcat exploratory well drilled in 1998, lies within the study region at coordinates 27° 37' 38.111 N, 10° 41' 57.2" E (Figure 1C). This well, reaching a total depth of 5575 feet, produces gas from Ordovician sandstones encountered between 4856 and 5015 feet. Precise static corrections in this region are exceptionally demanding due to the severe dune topography and the unique properties of the sand. Its arid conditions contribute to low seismic velocity, while potential hydrocarbon saturation further complicates the calculation process.

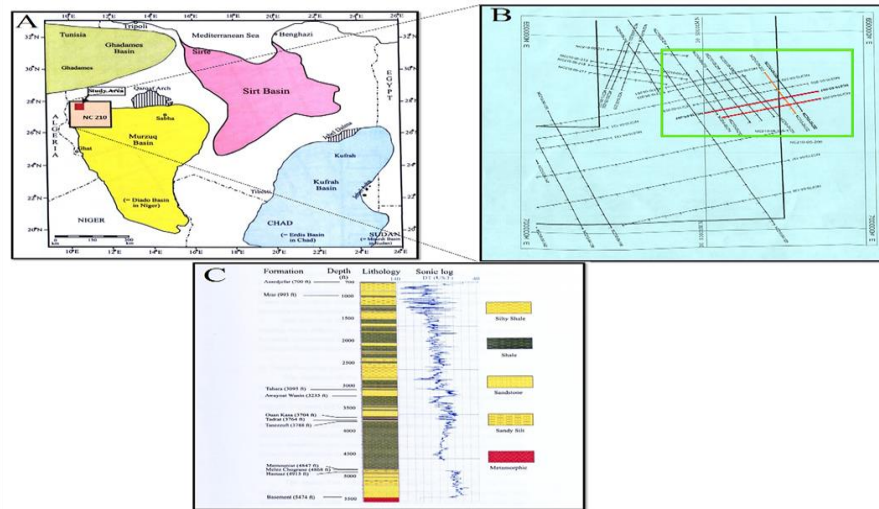


Fig. 1: the Concession N 210 (A) the Seismic Lines (B) Lithological Sequence and Sonic Log Recorded in Well F 1-NC 210 (C).

Methodology

Static corrections constitute a critical processing step for land seismic data, especially in regions characterized by rugged topography and pronounced near-surface velocity variations. Seismic lines NC202, NC207, and NC209 traverse areas with substantial sand dune coverage, resulting in a highly heterogeneous near-surface velocity field. To address this challenge, four uphole surveys were conducted at approximately 4-kilometer intervals along seismic lines NC210, NC202, and NC207. In contrast, two uphole surveys were established at similar intervals along seismic line NC210-209.

Static corrections, as defined by Sheriff (1991), were applied to seismic data to counteract the influence of factors such as elevation, weathering layer thickness, and weathering velocity relative to a specified datum. The primary goal of this study is to establish the theoretical reflection arrival times that would be observed under idealized conditions—a flat, horizontal surface devoid of weathering or low-velocity materials. These corrections are typically derived from uphole data, refraction first breaks, and/or event smoothing techniques. Comprehensive knowledge of source and receiver locations, elevations, and the velocity and thickness parameters of near-surface layers is essential for achieving a statistically robust solution.

2.1. Basic method of weathering and elevation travel time

Fig (2) shows a near-surface profile with the location of a source, or receiver, at point A on the surface. The weathering travel time (t_{WA}) is the weathering thickness that can be obtained by the division of (Z_A) and the weathering velocity (V_W) at location A (1),

$$t_{WA} = Z_A / V_W \quad (1)$$

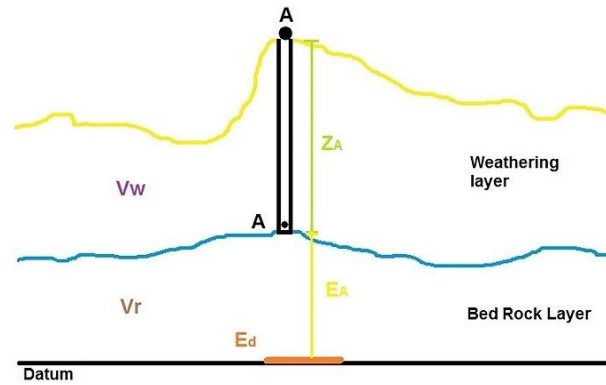


Fig. 2: Computation of Datum Static Corrections with the Source or Receiver at the Surface.

If there is more than one weathered layer, the weathering travel time is the sum of individual layer travel times, each of which is computed from its thickness and velocity. Then elevation travel time is computed by using (2) where elevation travel time (t_{EA}) is the thickness of sub weathered layer above the datum divided by the replacement or datum velocity (v_r)

$$t_{EA} = (EA - ZA - Ed)/V_r \quad (2)$$

Where:

EA = elevation of the source (or receiver) at A.

ZA = thickness of the weathered layer at A.

Ed = elevation of the reference datum.

V_r = replacement (or datum) velocity.

If more than one weathered layer is present, the symbol (ZA) in equations (1 and 2) refers to the total thickness of all the weathered layers. Thus, the total datum static correction, (t_A), is formed from the sum of weathering and elevation travel times. It is a known convention that static correction is negative for sources and receivers above the datum, as shown:

$$t_A = - (t_{WA} + t_{EA}) \quad (3)$$

The low velocity layer is characterized by the following features (Sheriff 1989, pp. 338-339):

- large impedance contrast with material below it,
- acts as a variable low pass filter. Therefore, it would produce a change in upgoing reflected waveform,
- ray paths in the low velocity layer are nearly vertical irrespective of their directions below it,
- thickness and velocity vary - as a result travel time of waves passing through it would vary.

2.2. Uphole survey

Accurately determining the thickness and velocity properties of the weathering layer presents a significant challenge in seismic data acquisition. The uphole survey method (Figure 3) is a widely employed technique to address this issue. Involves drilling boreholes to depths ranging from 50 to 100 meters at predetermined intervals along the seismic line, typically starting at approximately 1-kilometer spacing, with exact intervals adjusted based on specific survey needs (Dong and Xiang-Yun, 2006). A seismic source, such as a vibroseis truck or dynamite charge in a shallow shot hole, is positioned a few meters from the borehole's top. A geophone array is then lowered into the borehole to record the travel times of direct wave first arrivals.

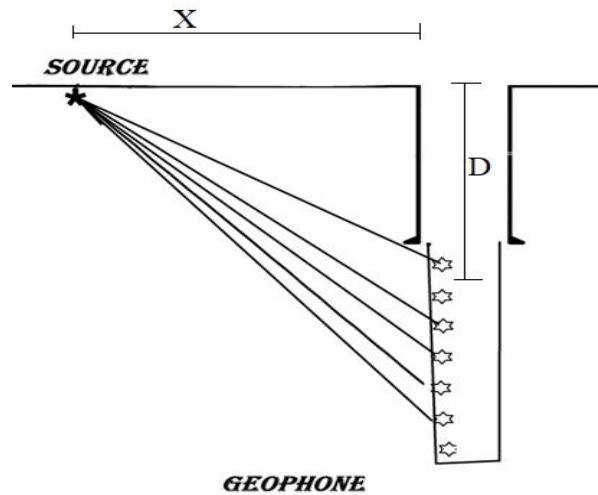


Fig. 3: Shows Uphole Survey.

To accurately determine vertical uphole times, it is essential to apply corrections to the measured slant travel times. These corrected vertical travel times subsequently serve as the basis for estimating near-surface layer velocities. Equation (4) illustrates the mathematical relationship between vertical uphole time (T) and measured (inclined) uphole time (t).

$$T = [t(D + E) / \{(D + E)^2 + X^2\}^{0.5}] \quad (4)$$

Where:

D= the depth from the top of the uphole to the down-hole source or receiver.

X= offset (horizontal distance between the top of the up hole and the surface source or receiver).

E= elevation of the surface source or receiver minus the elevation at the top of the uphole.

1. Estimating field statics

Figure 4 illustrates a representative uphole analysis from a borehole situated on a sand dune's upper flank. A vertical uphole time versus depth plot, featuring linear regressions, was generated. The slope of each linear segment corresponds to the velocity of a specific layer, while the intersections (knee points) define layer interfaces. Layer thicknesses are subsequently calculated based on these interface depths.

To quantify weathering and sub-weathering layer properties directly, each uphole was modeled as a three-layer system (Figure 5). This approach yielded thicknesses for the top two layers and interval velocities for all three layers. Table 1 summarizes the calculated datum static corrections (weathering and elevation components) for all uphole stations along seismic lines NC210, 202, and 207.

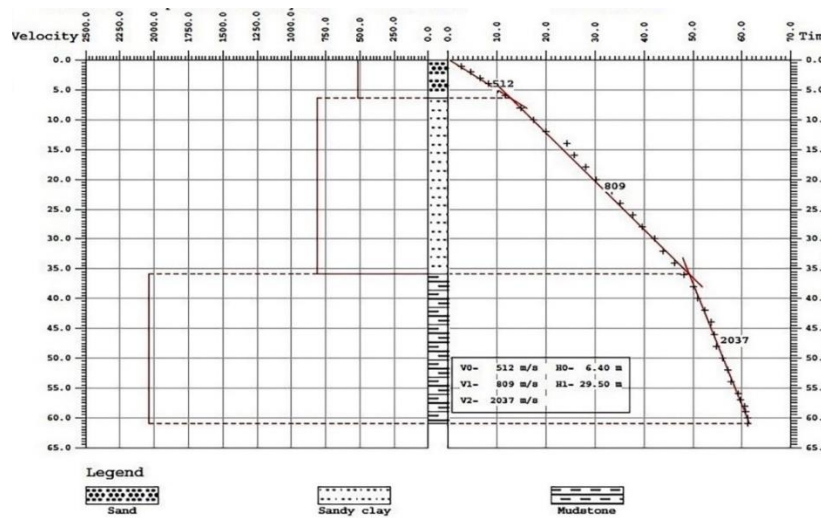


Fig. 4: Interpretation of Uphole (UH05_001_209) Survey Data Depicting Three Geologic Layers.

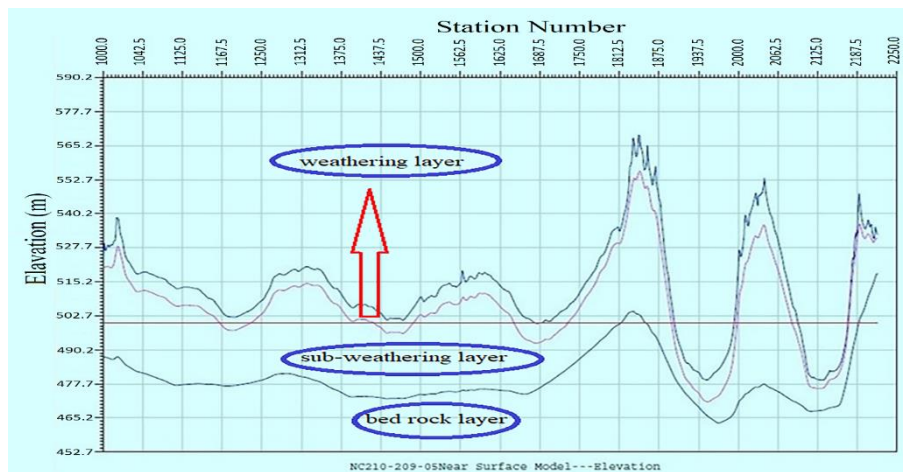


Fig. 5: Near-Surface Layer Thicknesses Along Part of Seismic Line NC210-209, Interpolated between Line Intersections and Control Points and between Control Points and Upholes, for the Conventional Method of Estimating Field Statics.

Table 1: Computation of Datum Static Corrections (Weathering and Elevation Corrections) at the Upholes Along Seismic Lines NC210-(202, 207 and 209)

Name of Uphole	009	007	008	010	002	005	032	034	001	006
Ele(m) (surface Elevation)	530.7	506.4	509.9	520	521.1	517.0	498.5	507.3	513	517.8
Datum	500	500	500	500	500	500	500	500	500	500
Z1 (Thickness layer 1)	3.9	4.9	4.8	5.7	15.4	7.4	2.6	2.8	6.4	5.5
Z2 (Thickness layer 2)	17.5	28.7	29.9	35.7	27.4	35.5	13.6	27.6	29.5	40.7
Z3 (Thickness layer3)	33.2	-	-	-	-	-	-	-	-	-
V1 (weathering velocity layer 1)	370	593	473	488	657	617	398	340	512	472
V2 (weathering velocity layer 2)	763	834	775	789	877	834	1014	792	809	880
V3 (weathering velocity layer 3)	2069	-	-	-	-	-	-	-	-	-
Vr (replacement velocity)	904	2092	2035	2105	2002	2109	2448	2065	2037	2289
Ele-(z1+z2)-Datum	-23.9	-27.3	-24.9	-21.3	-21.7	-25.8	-17.7	-23.2	-22.9	-28.3
weathering correction1 Z1/V1	10.6	8.4	10.2	11.6	23.4	11.9	6.6	8.3	12.5	11.6
weathering correction2 Z2/V2	22.9	34.4	38.7	45.2	31.3	42.6	13.4	34.9	36.5	46.3

weathering correction3 Z3/V3	16	-	-	-	-	-	-	-	-	-
Elevation correction	-26	-13	-12.2	-10	-10.8	-12.2	-7.2	-11.2	-11.3	-12.4
Datum correction	-23.1	-29.8	-36.7	-46.8	-43.8	-42.3	-12.7	-31.9	-37.7	-45.5

3.1. Gain corrections

Woodside provided field tapes and observer reports for the three seismic lines. Data in SEG-Y format was extracted from these tapes or disks and transformed into a structured file format suitable for processing operations. This standardized format facilitates data transfer between different processing contractors.

Upon shot initiation, seismic waves propagate spherically in three dimensions. This spherical divergence phenomenon attenuates energy as it propagates away from the source. Notably, higher frequencies are more susceptible to rock absorption compared to lower frequencies (Rothman, 1986). Consequently, seismic reflections from deeper geological structures are received at the geophone with weaker amplitudes relative to near-surface reflections. To amplify these weaker signals, a gain function is applied during processing.

3.2. Test function gain

To apply time-variant gain, the time value (in seconds) associated with each data sample is initially raised to a user-specified exponential power. The resulting value is then multiplied by the corresponding sample amplitude, as illustrated in Figure 6. This process involves scaling trace samples by first exponentiating the time value based on the user-defined GAIN EXPONENT parameter within the General Parameters set and subsequently multiplying the outcome by the sample amplitude.

$$A_o(t) = A_i(t) t^x \tag{5}$$

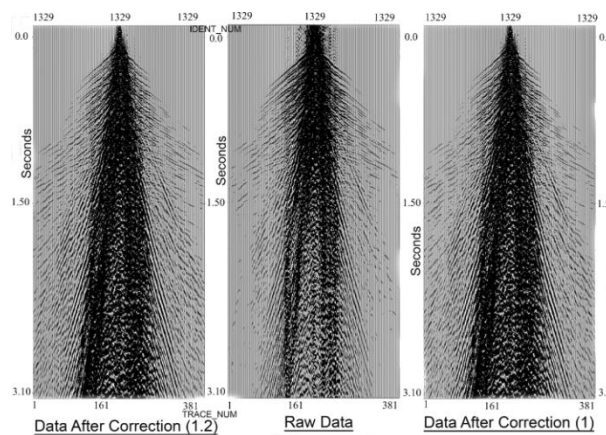
$A_o(t)$ = Amplitude of output trace sample at time t.

$A_i(t)$ = Amplitude of input trace sample at time t

t = Time in seconds.

x = Value of GAIN EXPONENT.

Fig (6) shows four tests have been done with different values of GAIN EXPONENT (1, 1.2, 1.8 and 2) the difference between raw data and tested data.



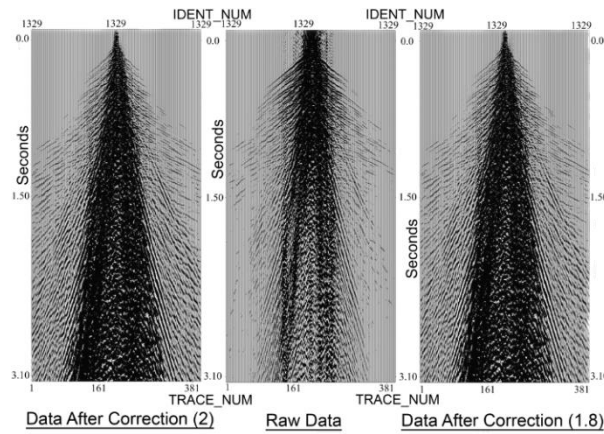


Fig. 6: Raw Data and Tested Data with Gain Exponent Values (1, 1.2, 1.8, 2).

The Geometric Spreading Amplitude Compensation

Seismic data typically undergoes either normal or inverse geometric spreading correction, contingent upon the availability of trace header geometry data. While absorption in rocks is purportedly linked to the first power of frequency, its relationship with the square of frequency is more prevalent in liquids (Anstey, 1977). The magnitude of absorption loss stemming from friction is notably higher in hard rocks compared to fluid-saturated formations, where frictional resistance is comparatively minimal due to the fluid's low viscosity (Gregory, 1977).

Geometric spreading amplitude compensation addresses the amplitude decay characteristic of primary seismic waves emanating from a point source. However, this process can lead to excessive compensation for water-bottom and peg-leg multiples. Figure 7 presents a dataset that has undergone geometric spreading amplitude correction.

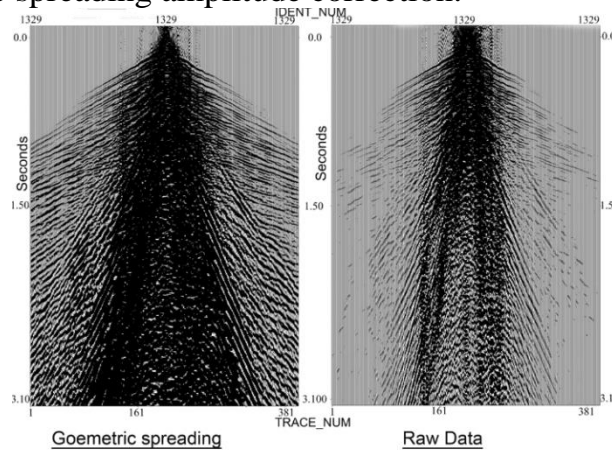


Fig. 7: Shows A Row Data and Tested Data with Geometric Spreading Amplitude.

The Residual Amplitude Analysis Compensation (RAAC)

Preserving genuine amplitude characteristics within seismic data often conflicts with the necessity of applying data-dependent scaling to manage the wide dynamic range of seismic data. The RAAC method offers a compromise by statistically preserving prominent amplitude anomalies, such as bright spots, while enabling data scaling. In the analytical phase of RAAC, the RMS amplitude of multiple time windows is computed for each trace, as depicted in Figure 8. The reciprocal of this calculated RMS amplitude constitutes the RAC value for each window.

The temporal midpoint of each time window serves as the reference point for its corresponding RAC value. By establishing the spatial (X-Y) and temporal coordinates of each RAC value, both spatial and temporal smoothing can be applied to these values. The subsequent application

phase involves interpolating the smoothed RAC values to every data sample and multiplying these interpolated scalars with the input traces.

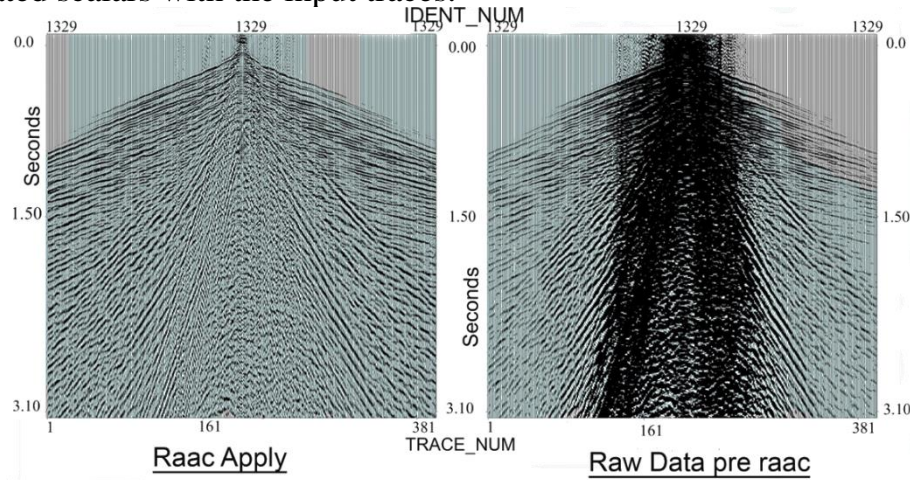


Fig. 8: Shows A Raw Data before RAAC and Data after RAAC Apply.

3.3. Seismic data processing

Seismic data processing for three lines was conducted at Western-Geco (WG) utilizing the Omega software package. The Anomalous Amplitude Attenuation (AAA) filter effectively suppressed random noise within the dataset. Simultaneously, the FK filter, applied with a velocity of 1500 m/s, successfully eliminated ground roll, airwave, and cable jerk interference. Deconvolution parameters were optimized with an operator length of 240 ms and a gap of 32 ms.

The concept of common depth point (CDP) gathers equates to common midpoint (CMP) gathers at the surface under idealized conditions of horizontal reflectors and constant velocity. Nonetheless, in the presence of complex subsurface geology characterized by varying dip angles, CMP trace arrays are essential for precise RMS velocity estimation (Levin, 1971). Consequently, when encountering dipping reflectors, the distinction between CDP and CMP gathers becomes crucial, with CMP being the preferred terminology. The migration process effectively transforms CDP gathers into CMP-equivalent gathers through an up-dip shift.

CMP stacking constitutes a pivotal step in conventional seismic reflection processing, as it enhances the signal-to-noise ratio by attenuating random noise, coherent noise, and multiple reflections with distinct moveout characteristics. For lines 202, 207, and 209, the identical geophone and shot point intervals resulted in a maximum fold coverage of 200 with a total of 400 recording channels.

3.4. Velocity analysis

Stacking velocity constitutes a critical parameter influencing stack quality. These velocities are employed to rectify Normal Moveout (NMO) distortions, aligning reflections within Common Midpoint (CMP) gathers prior to stacking. Two primary methods exist for estimating stacking velocity (Figure 9).

The Constant Velocity Stack (CVS) method entails selecting the velocity that optimizes stack response at a specific CMP event time. Iterative application of this approach across multiple reflectors establishes a velocity function suitable for NMO corrections (Al-Yahya, 1989). This method involves individually applying NMO velocities to each reflector before collectively applying them to achieve a linear velocity trend.

The velocity spectrum method offers an alternative approach by identifying semblance peaks within CMP panels to determine optimal stacking velocity. While effective for data containing multiple reflections, this method exhibits limitations when dealing with complex subsurface structures.

Seismic lines NC210, 202, and 207 primarily utilized these two methods for stacking velocity estimation.

3.5. Application to a seismic line crossing sand dune

Figure 9 presents the stacked section of seismic line 209, which clearly exhibits the impact of traversing sand dunes. Increased travel times of reflected events within this region generate spurious subsurface structures, a phenomenon attributed to residual static errors (Steeple et al., 1990).

The conventional processing workflow, outlined in Figure 10, encompasses RAAC gain correction, FK filtering of common shot gathers, predictive deconvolution, NMO correction, and stacking (Cox, 1999). While this approach effectively reduces noise, it fails to completely eliminate false structures beneath the sand dunes, where signal quality is compromised. Surface elevation and conventional field statics were determined for the seismic line.

A comparative analysis was conducted using the same processing sequence on line 209, but incorporating uphole statics (datum statics) instead of conventional field statics (Figure 11). This comparison revealed a significant reduction in false structures beneath the sand dunes, although overall signal-to-noise ratio remained suboptimal in this area. Subsequent application of automatic statics programs markedly improved signal quality, enabling refined velocity analysis and CMP trim statics. In contrast to the conventional approach, which failed to adequately address the false structures evident in Figure 10, the uphole static correction method yielded a more accurate representation (Wenxi and Chunyan, 2007).

Upon applying uphole static corrections (datum statics) to seismic lines NC210, 202, and 207, a comparative analysis of the final corrected seismic lines (Figure 12) with rapid interpretation notes from line 202 clearly indicates a vertical offset within the reflector across a fault zone.

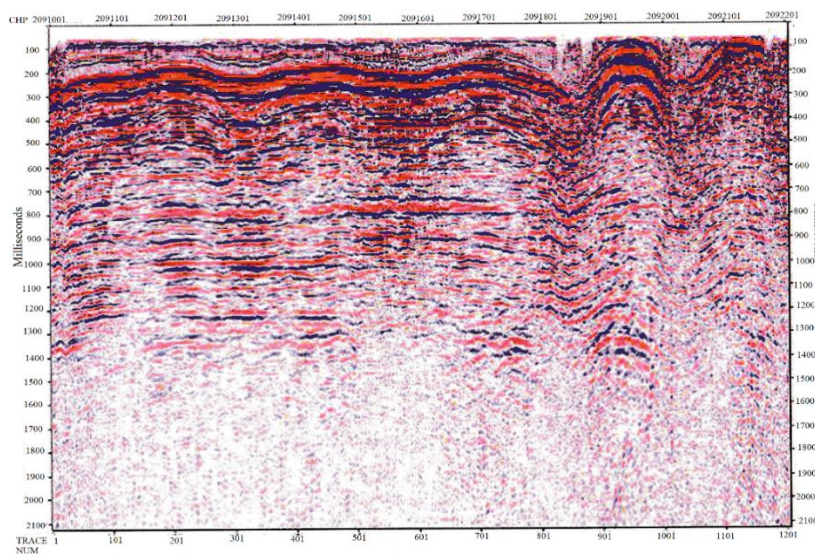


Fig. 9: Shows Stack Section to Seismic Line 209.

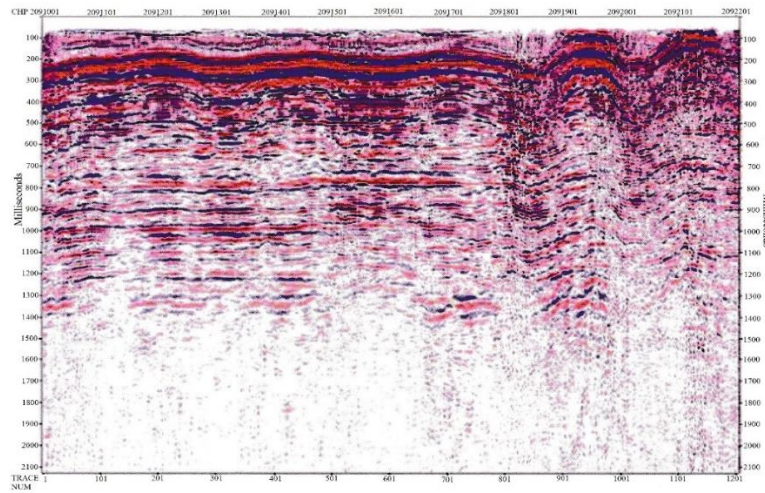


Fig. 10: Shows Elevation Static Correction to Seismic Line 209.

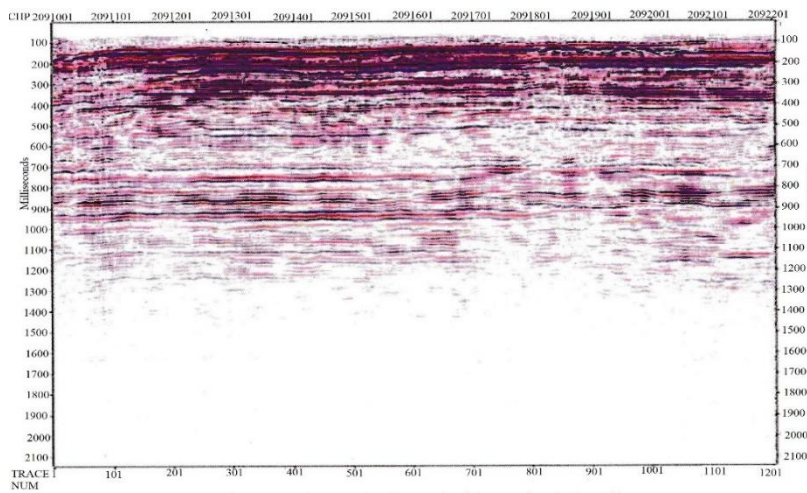


Fig. 11: Shows Uphole Static Correction (Datum Statics) to Seismic Line 209.

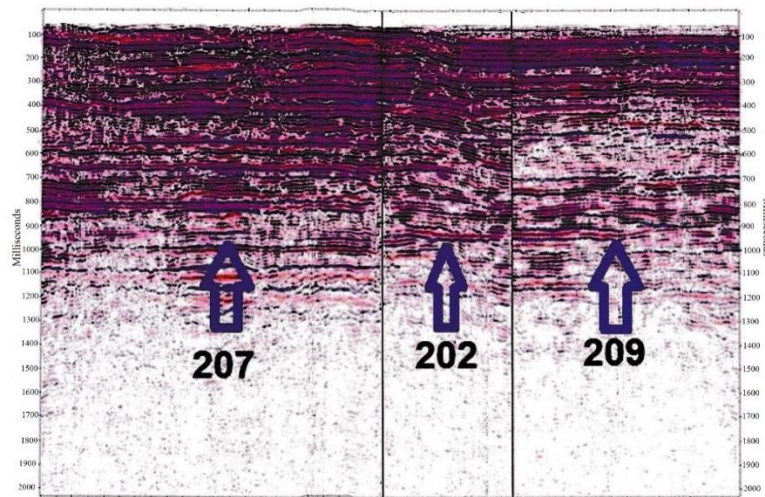


Fig. 12: Show Intersection Between Final Correction to Seismic Lines (202,207,209).

2. Conclusion

This research investigates the challenges posed by static problems on seismic reflection profiles within the sand dune terrain of Concession N210, western Libya. The study employs the uphole static method to address these issues. Three seismic lines, totaling approximately 38 kilometers, traversing sand dune formations, were processed using Omega software by Western Geco. To calculate vertical uphole times, measured slant travel times underwent correction. Each uphole was modeled as a three-layer system, with thicknesses determined for the top two layers and interval velocities calculated for all three layers relative to a 500-meter datum. Subsequently, datum static corrections, encompassing weathering and elevation components, were computed for all uphole stations across the three lines. A comprehensive evaluation of gain correction techniques was conducted using real data from NC210. Time-function domain testing yielded unsatisfactory results in terms of resolving subsurface structures. Conversely, geometric spreading amplitude compensation effectively mitigated noise, producing acceptable horizontal data. However, residual noise remained evident. The application of RAAC to raw data demonstrated superior noise attenuation and amplitude correction capabilities compared to other methods. The Anomalous Amplitude Attenuation (AAA) filter effectively suppressed random noise, including ground roll, airwave, and cable jerk interference.

Two primary methods were employed for stacking velocity estimation: constant velocity stack (CVS) and velocity spectrum analysis. While CVS offers simplicity, the velocity spectrum method, particularly suited for data with multiple reflections, provides enhanced accuracy.

Numerous static correction methods exist for improving seismic stack sections. Among these, uphole statics have demonstrated superior performance compared to elevation statics, especially in sand dune environments (Jiang, 2008). The results from processing seismic lines crossing the sand dunes show that the datum static method gives much better results than the conventional field static method (Yoo and Haug, 1986). No faults were present on the line crossing the sand dunes, but there was a fault on the line 202 located between sand dunes.

Similar care will have to be taken around fault locations when processing seismic lines that cross over sand dunes with the uphole statics (datum statics) method.

3. Highlights

- Sand dunes present substantial logistical and technical challenges to seismic reflection exploration.
- Static corrections are applied to seismic data to account for variations in elevation, weathering layer thickness, weathering velocity, and datum reference.
- This study compares the efficacy of different methods in addressing seismic challenges posed by sand dunes in southwestern Libya.
- Results from processing seismic lines traversing sand dunes demonstrate the superior performance of the datum static method over the conventional field static approach. On behalf of all the co-authors, the corresponding author states that there is no conflict of interest.

References

- [1] Al-Yahya, K. (1989). Velocity analysis by iterative profile migration. *Geophysics*, 54(6), 718-729. <https://doi.org/10.1190/1.1442699>.
- [2] Anstey AN (1977) Seismic interpretation, the physical aspects, record of short course "The new seismic interpreter". IHRDC of Boston, Massachusetts.

- [3] Aziz, A. 2000. Stratigraphy and hydrocarbon potential of the Lower Palaeozoic Succession of License NC-115, Murzuq Basin SW Libya in: Geological Exploration in Murzug Basin (eds M.A. Sola and D. Worsley). 349-368. Elsevier. <https://doi.org/10.1016/B978-044450611-5/50018-0>.
- [4] Cox, M. (1999). *Static corrections for seismic reflection surveys*. Society of Exploration Geophysicists. <https://doi.org/10.1190/1.9781560801818>.
- [5] Fello, N.M. 2001, Depositional Environments, Diagenesis and Reservoir Modelling of Concession NC115, Murzug. Basin SW Libya, Ph.D. thesis, University of Durham, U.K.
- [6] Gregory AR (1977) Aspects of rock physics from laboratory and log data that are important to seismic interpretation. AAPG Mem 26:15–46.
- [7] Grubic, A., Dimitruevic, M., Galecic, M., Jakovljeic, Z., Komarnicki, S., protic, D., Radulovic, P. and Ronceric, G. 1991. Stratigraphy of western Fazzan, SW Libya. In: The Geology of Libya (eds MJ. Salem and M.N. Belaid), 1529-1565. Academic Press.
- [8] HAN Xiao-li1, YANG Chang-chun1, MA San-huai1, QIN Hong-guo2 (1. Institute of Geology and Geophysics Chinese Academy of Sciences, Beijing 100029, China; 2. BGP Inc., CNPC, Zhuozhou 072751, China); Static of tomographic inversion by first breaks in complex areas[J]; Progress in Geophysics; 2008-02.
- [9] LEI Dong~1, 2 HU Xiang-yun~2 (1. China Southern Petroleum Exploration & Development Corporation, Guangdong, Guangzhou 510240, China) (2. Institute of Geophysics and Geomatics, China University of Geosciences, Wuhan 430074, China); Review of Seismic Tomography Methods[J]; Journal of Seismological Research; 2006-04.
- [10] Levin, F. K. (1971). Apparent velocity from dipping interface reflections. *Geophysics*, 36(3), 510-516. <https://doi.org/10.1190/1.1440188>.
- [11] NOC (National Oil Corporation), Internal Report, 2013.
- [12] Pierobon, E.S.T. 1991. Contribution to the stratigraphy of the Murzug Basin, SW Libya. In: The Geology of Libya (eds M.J. Salem and M.N. Belaid), 1767-1784, Elsevier.
- [13] Rothman, D. H. (1986). Automatic estimation of large residual statics corrections. *Geophysics*, 51(2), 332-346. <https://doi.org/10.1190/1.1442092>.
- [14] Sheriff, R. E. (1989). *Geophysical methods*. Prentice Hall.
- [15] Sheriff, R.E. 1991. *Encyclopedic Dictionary of Exploration Geophysics*, 3rd edn. Society of Exploration Geophysicists, Tulsa.
- [16] Steeples, D. W., Miller, R. D., & Black, R. A. (1990). Static corrections from shallow-reflection surveys. *Geophysics*, 55(6), 769-775.
- [17] Ushah, A.M. 2004. static problems Due to sand dunes in NC 151, Western Libya A thesis submitted in partial fulfillment of the requirements for the degree of Doctor of Philosophy. <https://doi.org/10.1190/1.1442889>.
- [18] WU Chang-jiang: A New and Simple Curve Equation for Correcting Dune Seismic Data[J]; Journal of Oil and Gas Technology; 2008.
- [19] Wu Wenxi1 and Liang Chunyan2 1 Exploration Department of Petro China Tuha Oil-field Company, Hami City, Xinjiang Uygur Autonomous Region 839009; 2 Petro China Tuha Petroleum Exploration & Development Headquarters, Hami City, Xinjiang Uygur Autonomous Region 839009; Tomographic Inversion and Static Correction of First Break in Surface Model and Their Application in Tuha Basin[J]; China Petroleum Exploration; 2007.
- [20] Yoo, W. S., & Haug, E. J. (1986). Dynamics of flexible mechanical systems using vibration and static correction modes. <https://doi.org/10.1115/1.3258733>.